Improvement of the cardiovascular effect ssof methyldopa by complexation with Zn(II): Synthesis, characterization and mechanism of action

Agustin Bruno Actis Dato, Valeria R. Martinez, Jorge O. Velez Rueda, Enrique L. Portiansky, Verónica De Giusti, Evelina G. Ferrer, Patricia A.M Williams

PII: S0946-672X(23)00203-1

DOI: https://doi.org/10.1016/j.jtemb.2023.127327

Reference: JTEMB127327

To appear in: *Journal of Trace Elements in Medicine and Biology*

Received date: 19 August 2023
Revised date: 3 October 2023
Accepted date: 19 October 2023

Please cite this article as: Agustin Bruno Actis Dato, Valeria R. Martinez, Jorge O. Velez Rueda, Enrique L. Portiansky, Verónica De Giusti, Evelina G. Ferrer and Patricia A.M Williams, Improvement of the cardiovascular effect ssof methyldopa by complexation with Zn(II): Synthesis, characterization and mechanism of action, *Journal of Trace Elements in Medicine and Biology,* (2023) doi:https://doi.org/10.1016/j.jtemb.2023.127327

Improvement of the cardiovascular effect of methyldopa by complexation with Zn(II): Synthesis, characterization and mechanism of action

Agustin Bruno Actis Dato[1], Valeria R. Martinez[2,*], Jorge O. Velez Rueda[2], Enrique L. Portiansky[3], Verónica De Giusti[2], Evelina G. Ferrer[1], Patricia A.M Williams[1,*]

[1] CEQUINOR-CONICET-CICPBA-UNLP, Facultad de Ciencias Exactas, Universidad Nacional de La Plata, Bv. 120 N◦ 1465, 1900 La Plata, Argentina

[2] CIC-CONICET-UNLP, Facultad de Médicas, Universidad Nacional de La Plata, 60 y 120, 1900 La Plata, Argentina

[3] Laboratorio de Análisis de Imágenes, Facultad de Ciencias Veterinarias, Universidad Nacional de La Plata, 60 y 118, 1900 La Plata, Argentina

* Corresponding authors. Tel +54 0221 445-4393;

e-mail: williams@quimica.unlp.edu.ar

varomart@hotmail.com

Abstract

Background: the antihypertensive drug α-methyldopa (MD) stands as one of the extensively used medications for managing hypertension during pregnancy. Zinc deprivation has been associated with many diseases. In this context, the synthesis of a Zn coordination complex $[Zn(MD)(OH)(H_2O)_2].H_2O$ (ZnMD) provide a promising alternative pathway to improve the biological properties of MD.

Methods: ZnMD was synthesized and physicochemically characterized. Fluorescence spectral studies were conducted to examine the binding of both, the ligand and the metal with bovine serum albumin (BSA). MD, ZnMD, and $ZnCl_2$ were administered to

spontaneous hypertensive rats (SHR) rats during 8 weeks and blood pressure and echocardiographic parameters were determined. *Ex vivo* assays were conducted to evaluate levels of reactive oxygen species (ROS), thiobarbituric acid reactive substances (TBARS), and nitric oxide (NO). Cross-sectional area (CSA) and collagen levels of left ventricular cardiomyocytes were also assessed. Furthermore, the expression of NAD(P)H oxidase subunits ($gp91^{phox}$ and $p47^{phox}$) and Superoxide Dismutase 1 (SOD1) was quantified through western blot analysis.

Results: The complex exhibited a moderate affinity for binding with BSA showing a spontaneous interaction (indicated by negative ΔG values) and moderate affinity (determined by affinity constant values). The binding process involved the formation of Van der Waals forces and hydrogen bonds. Upon treatment with MD and ZnMD, a reduction in the systolic blood pressure in SHR was observed, being ZnMD more effective than MD (122 ± 8.1 mmHg and 145 ± 5.6 mmHg, at 8^{th} week of treatment, respectively). The ZnMD treatment prevented myocardial hypertrophy, improved the heart function and reduced the cardiac fibrosis, as evidenced by parameters such as left ventricular mass, fractional shortening, and histological studies. In contrast, MD did not show noticeable differences in these parameters. ZnMD regulates negatively the oxidative damage by reducing levels of ROS and lipid peroxidation, as well as the cardiac NAD(P)H oxidase, and increasing SOD1 expression, while MD did not show significant effect. Moreover, cardiac nitric oxide levels were greater in the ZnMD therapy compared to MD treatment.

Conclusion: Both MD and ZnMD have the potential to be transported by albumin. Our findings provide important evidence suggesting that this complex could be a potential therapeutic drug for the treatment of hypertension and cardiac hypertrophy and dysfunction.

Keywords: Zn-α-methyldopa; SHR rats; Hypertension; Cardiovascular disease

Graphical abstract

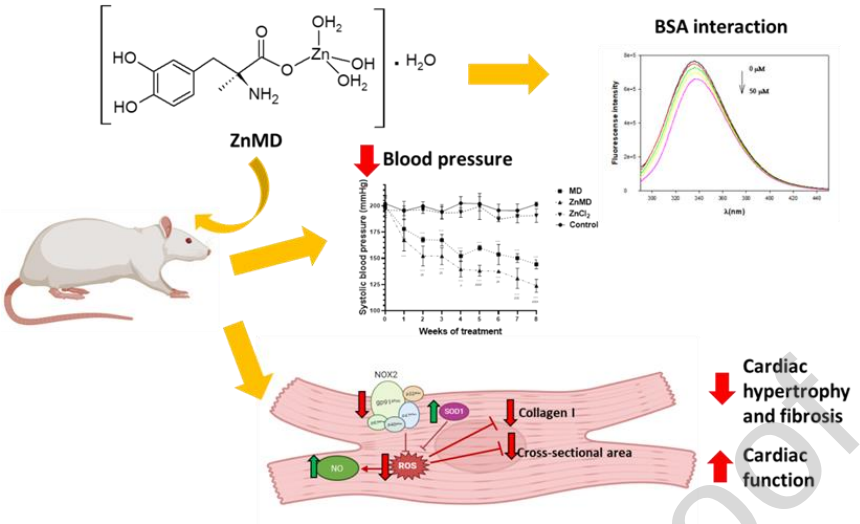

1. Introduction

Hypertension is one of the major risk factors for cardiovascular diseases, such cerebrovascular and heart attack. High blood pressure is the major cause of premature death, and the World Health Organization has reported that 1.28 billion adults aged 30-79 years worldwide have hypertension [1]. Because of uncontrolled hypertension and consequent pressure overload, left ventricular hypertrophy (LVH) develops as a compensatory mechanism to maintain heart function. This hypertrophic response increases the cardiomyocyte size, the myocardium enlarges, the extracellular matrix alters with collagen buildup and fibrosis occurs, which results in the stiffening of the ventricular wall, leading to contraction and relaxation impairment [2]. Also, an imbalance in the renin-angiotensin-aldosterone system and sympathetic nervous system, as well as endothelial dysfunction, inflammatory response, and the generation of reactive oxygen species (ROS) lead to eventually progressing to maladaptive remodeling and pushing the heart into a decompensated state [3].

Despite interventions and programs to promote cardiovascular health through lifestyle changes and the use of a well-balanced diet, this health problem persists, and it is necessary to pave the way for better treatment strategies that target the factors involved in the maladaptive progression.

Most antihypertensive drugs were designed to target specific mechanistic pathways involved in the development of hypertension. These medications include: 1) Beta-blockers, which reduce the amount of blood pumped through the arteries. 2) Diuretics that help the kidneys to remove excess sodium from the body. 3) Angiotensin-converting enzyme inhibitors (ACE inhibitors), which inhibit the effects of angiotensin that cause blood vessel and artery constriction (e.g., enalapril). 4) Angiotensin II receptor blockers (ARBs), which block the action of angiotensin (e.g., sartans). 5) Calcium channel blockers, which prevent excess calcium from entering the smooth muscles of arterial vessels, thus reducing contraction and blood pressure (e.g., nitrendipine and nisoldipine). 6) Alpha-2 agonists, which relax muscles and lower blood pressure (e.g., α-methyldopa, hydroxy-α-methyl-L-tyrosine). 7) Renin inhibitors, which specifically target the rate-limiting step of the renin-angiotensin system (e.g., aliskiren) [4].

α-Methyldopa (MD), shown in Fig. 1, primarily acts within the central nervous system as an α_2-adrenergic agonist. It is taken up by adrenergic neurons and undergoes decarboxylation and hydroxylation to form the false transmitter α-methylnoradrenaline. However, compared to noradrenaline, it is less active on α-receptors and therefore less effective in causing vasoconstriction [5]. In order to achieve a hypotensive effect with MD, high doses are typically required [6]. However, these high doses can lead to adverse effects on the nervous system, including symptoms such as dizziness, drowsiness, tiredness, dry mouth, headache, and depression [7]. Despite these potential side effects, MD is still widely used for managing hypertensive disorders during pregnancy, such as gestational hypertension and (pre)eclampsia, and it is notable for not causing any teratogenic effects [8]. To improve the beneficial effects of the drug and enable its administration at lower concentrations, its chemical structure can be modified through metal complexation.

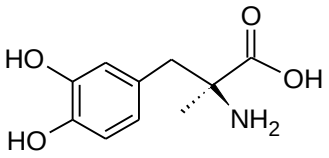

Fig. 1. Structure of α-methyldopa

In the literature, there are examples of coordination complexes formed between biometals and certain antihypertensive drugs. However, the biological effects of these complexes have been studied in only a limited number of cases [9–12].

To our knowledge, there are no reports available on the biological effects of solid coordination complexes involving $\alpha_2$agonists as ligands. Therefore, conducting such studies could provide a promising alternative pathway for the development of new families of antihypertensive compounds.

Zinc is the second most abundant trace biometal found in the human body, and it serves multiple essential functions, including catalytic, structural, and regulatory roles. These functions are crucial for the growth and development of all living species [13]. Moreover, studies have demonstrated that dietary zinc deprivation can increase cellular susceptibility to oxidative stress, thereby disrupting various physiological and metabolic functions. Consequently, many diseases have been associated with zinc deficiency [14]. Furthermore, because of its d^{10} electronic structure, Zn(II) can adopt a variety of coordination geometries, including those with coordination numbers of 4 (tetrahedral), 5 (pyramidal), and 6 (octahedral). The specific coordination geometry and the ligands involved (with functional groups containing sulfur (S), nitrogen (N) or oxygen (O) atoms) can influence its conformation. These modifications have the potential to alter its biological properties. [15].

Fig. 1 illustrates that α-Methyldopa (MD) exhibits various coordination sites capable of chelating with metal ions. Solution studies involving methyldopa and copper(II) cations, conducted using potentiometric techniques, have described different coordination modes under different experimental conditions. These modes include N,O coordination involving

NH_2 and COO^- groups, as well as O,O coordination involving the catechol moiety [16] Similar to other studies utilizing thermodynamic measurements [17], the investigations have provided insights into the behavior of copper(II) complexes formed by methyldopa, methyltyrosine, and catechol in aqueous solutions. According to reports, it has been concluded that N,O coordination occurs at low pH values, while in alkaline solutions, the catechol end of α-Methyldopa (MD) coordinates with the metal ion. While the drug can undergo instability in an alkaline environment due to the presence of the catechol system, it is possible to prevent this type of decomposition by working under a nitrogen atmosphere, even at high temperatures [18].

In the case of zinc(II) cations and related catechol compounds, studies have reported that chelation of L-dopa (3-(3,4-Dihydroxyphenyl)-L-alanine) occurs through the amino and carboxylic groups within a pH range of 6 to 9 [19]. During the experiment conducted with Zn^{2+}, H_2O_2, horse peroxidase, and L-dopa, the aromatic oxidation of the catechol ligand to the o-semiquinone radical was observed. These o-semiquinone radicals interacted with the metal ion, resulting in the carboxylate and amino groups being uncoordinated [20].

In the current study, we synthesized and characterized a solid Zn/α-methyldopa complex with a 1:1 stoichiometry, at pH 6.4, and demonstrated that the coordination mode N,O occurs. Bovine serum albumin was selected as the transport protein and the binding interactions with the ligand and the complex were studied by spectrofluorometric determinations. The biological effects of this new compound were evaluated in spontaneously hypertensive rats (SHR) to assess its antihypertensive and antihypertrophic properties. We investigated the heart function improvement by means of the decrease of LVH and fibrosis and the reduction of oxidative stress.

2. Materials and Methods

$ZnCl_2$ (Biopack, Argentina) and α-methyldopa (Saporiti, Argentina) were used as purchased. All other chemicals were of analytical grade and used as supplied. Elemental

analyses for carbon, nitrogen, and hydrogen were performed using a Carlo Erba EA 1108 analyzer. Zn contents were determined using the Zincon method (2-[2-[(Z)-N-[(E)-(6-oxo-3-sulfocyclohexa-2,4-dien-1-ylidene)amino]-C-phenylcarbonimidoyl]hydrazinyl] benzoic acid, Santa Cruz Biotechnology) [21]. Thermogravimetric (TG) determinations were conducted using a Shimadzu system (model TG-50) in an oxygen flow of 50 mL/min with a heating rate of 10 °C/min. The sample quantities ranged between 10 and 20 mg. FTIR spectra of powdered samples were measured using a Bruker IFS 66 FTIR-spectrophotometer from 4000 to 400 cm^{-1}. The samples were in the form of pressed KBr pellets. Electronic absorption and fluorescence spectra were recorded using a Shimadzu UV-2600/2700 spectrophotometer and a Shimadzu RF-6000 spectrofluorometer, respectively**.** Conductivity measurements were carried out using a TDS Probe 850.084 conductimeter. For the ^{1}H NMR measurements, a Bruker Ultrashield 600, 14.1 Tesla spectrometer was used. The measurements were performed in 100% DMSO-d_6 solution at 25 °C and at a frequency of 600 MHz. Tetramethylsilane was used as an internal standard to calibrate the chemical shift δ.

2.1. Preparation of ZnMD ([ZnMD(OH)(H_2O)$_2$].H_2O)

To a 10 mL solution of methyldopa (0.2 mmol) in methanol, 0.4 mL of a solution of $ZnCl_2$ (0.2 mmol) in methanol was added. The mixture was stirred for 10 min under nitrogen flow. Then, an aqueous 1 M solution of KOH has been added until the final pH reached a value of 6.4. The white solid formed was filtered, washed with methanol and dried under nitrogen flow.

Anal calc. for [ZnMD(OH)(H_2O)$_2$].H_2O ($C_{10}H_{19}O_8NZn$, MW: 346.65 g/mol): C, 34.6 %; H, 5.5 %; N, 4.0 %; Zn, 18.9 %; Found: C, 34.4 %; H, 5.4 %; N, 3.9 %; Zn, 19.0 %

Thermogravimetric analysis (Fig. S1) showed that three water molecules were lost up to 160 ºC (weight loss: exp., 15.5 %; calc., 15.6 %). The first water molecule, corresponding to hydration water, was removed at 60 ºC. The final residue, characterized by FTIR spectroscopy as ZnO [22]. (Fig. S2A) was 24.0 % at 900 ºC (calc. 23.5 %). The molar

conductance of the complex measured in H_2O, Λ_m = 12 (Ω^{-1} cm^2 mol^{-1}), suggested that the complex is non-electrolyte in nature.

2.2. In vitro bovine serum albumin (BSA) interaction

A solution of MD or ZnMD was prepared with 4.8 mL of Tris-HCl (0.1 M, pH 7.4), 10 µL of an aqueous 6 µM solution of BSA and 10 µL of a DMSO solution of the compounds. The final concentrations of the compounds ranged from 5 to 50 µM, while the buffer was used as a control. To assess the interaction of BSA with MD and ZnMD, the fluorescence intensity was measured using a luminescence spectrometer (Shimadzu 2600/2700) at 25 °C, 30 °C, and 37 °C, with excitation at 280 nm and emission at 350 nm. An incubation time of 20 min was determined, measuring the time at which a maximum of fluorescence intensity is achieved. Each sample was replicated three times independently. Before conducting the analysis, the BSA curves underwent deconvolution using Origin 2022 software. This process aimed to separate them from the overlapping spectra of either MD or ZnMD, enabling the extraction of the fluorescence peaks. The computational procedure involved subtracting the measured fluorescence spectra of either MD or ZnMD from the overall curve. All the experiments were performed in triplicate, each being repeated at least three times. Values are expressed as the mean ± standard error (SE).

2.3. Animals

The experimental protocols involving animal subjects were conducted following strict compliance with the guidelines stipulated by the National Institute of Health Guide for the Care and Use of Laboratory Animals (NIH Publication No. 85-23, revised 1996). Before undertaking the experiments, approval was granted by the Institutional Committee for the Care and Use of Laboratory Animals (CICUAL) at the Faculty of Medical Sciences of the National University of La Plata (Protocol number: T02-02-2023). Male spontaneously hypertensive rats (SHRs) weighing 200-300 g and aged 12 weeks were obtained from the Dr. Alfredo Lanari Medical Research Institute in Buenos Aires, Argentina. The 12-

week age was selected based on previous evidence of heart hypertrophy and hypertension development at this stage [23]. The rats were randomly allocated into four groups (n = 4-5 per group) using the resource equation method [24]. The animals were housed under standardized laboratory conditions with a temperature of 23 °C ± 1, a 12-h light and darkness cycle, and a humidity range of 60-70%. They were provided with *ad libitum* access to standard commercial rat-mouse chow (Cooperación, Buenos Aires, Argentina) and water.

MD, ZnMD, and $ZnCl_2$ were delivered to SHR rats via dietary administration using peanut butter balls, being a more cost-efficient alternative and inducing lower stress than traditional administration methods [25]. The rats consumed 200 mg/day of commercial peanut butter (Mani King, Buenos Aires, Argentina) containing 100.00 mg/kg/day of MD and the molar equivalent for ZnMD (164.12 mg/kg/day) and $ZnCl_2$ (64.52 mg/kg/day). The doses were selected based on previous reports of the antihypertensive effect of MD in SHR rats [26]. The control group received only the peanut butter without MD.

On a weekly basis, the experimental animals were weighed, and their systolic blood pressure was assessed using non-invasive tail-cuff plethysmography. To examine cardiac hypertrophy (CH), transthoracic two-dimensional M-mode echocardiography using a 7-MHz transducer was conducted on the rats at the beginning and end of the experimental protocol, under anesthesia with approximately 2-3% isoflurane in an oxygen flow. The measurements were carried out following the state-of-the-art guidelines provided by the American Society of Echocardiography [27]. The left ventricular mass (LVM) was calculated using the method outlined by Devereux and Reichek [28]. Additionally, the LVM index (LVMI) was determined as the ratio between the LVM and tibial length. Finally, fractional shortening was calculated using the following equation: ([(LVDd-LVDs)*100]/LVDd) (where LVDd is the diastolic left ventricular diameter and LVDs is the systolic left ventricular diameter).

At the 8-week of the experimental protocol, the animals were euthanized by administering a single dose of urethane (1 g/kg of body weight). After confirming the

absence of reflexes, the heart was excised and the left ventricle was separated. The tibia was removed to calculate the left ventricular mass/tibia length ratio. Subsequently, the left ventricles were divided and promptly frozen in liquid nitrogen, preserving them at a temperature of −80 °C. The frozen fractions were then utilized for measuring reactive oxygen species (ROS), thiobarbituric acid reactive substance (TBARS), nitric oxide (NO) and conducting immunoblot determinations. Coronal sections derived from the equator of the left ventricle were fixed in buffered 10% formaldehyde for 24 h. After fixation, the sections were paraffin-embedded, and thick (5 μm) sections were stained to facilitate histological analysis.

2.4. Preparation of Tissues for Ex Vivo Assays

To prepare tissue samples for *ex vivo* assays, a tissue fraction weighing approximately 250 mg was homogenized on ice with 1 mL of 40 mM Tris buffer per 100 mg of tissue using a Pro-Scientific Bio-gen Series Pro 2000 homogenizer. The resulting homogenate was used for quantifying ROS, TBARS and NO levels.

2.5. ROS, NO and TBARs Assessments

Next, 50 μL of homogenized samples were combined with 1 mL of 40 mM Tris buffer and H_2DCFDA (2′,7′-Dichlorofluorescin diacetate) probe at a final concentration of 10 μM (Mousavi et al., 2020). The resulting mixture was incubated for 30 min at 37 °C. To measure ROS levels, the samples were analyzed with an excitation wavelength of 485 nm and an emission wavelength of 535 nm, using a Varioskan spectrofluorometric multiplate reader.

Lipid peroxides, as reactive species of thiobarbituric acid, were quantified using previously established procedures [29] . 50 μL of tissue homogenate was mixed with 100 μL of 8.1% sodium dodecyl sulfate, 750 μL of 3.5 M acetate buffer (pH 3.5), 750 μL of 0.8% thiobarbituric acid, and 350 μL of water. The mixture was heated at 95 °C for 1 h, followed by cooling to room temperature. Next, 500 μL of water and 2.5 mL of a 15:1

mixture of n-butanol and pyridine were added, and the resulting solution was stirred and centrifuged at 4000 rpm. The absorbance of the organic phase was measured at 532 nm.

To indirectly determine the levels of nitric oxide (NO) as nitrite, the 2,3-diaminonaphthalene fluorimetry assay was utilized [30]. For this assay, 20 µL of freshly prepared 2,3-diaminonaphthalene (0.05 mg mL-1 in 0.62 N HCl) were mixed with 200 µL of the sample solution. After promptly mixing, the mixture was incubated at 25 °C for 15 min. The reaction was then stopped by adding 10 mL of 2.8 N NaOH. The fluorescent signal intensity generated by the reaction product, 1-(H)-naphthotriazole, was measured at 365 nm excitation and 450 nm emission wavelengths. Standard sodium nitrite solutions were freshly prepared prior to each measurement, and a standard curve relating fluorescence intensity to nitrite concentration was established.

2.6. Cross-sectional Area Determination of Left Ventricular Cardiomyocytes

The paraffin-embedded sections were stained with either hematoxylin eosin to determine the cross-sectional area (CSA) of cardiomyocytes. Histological images were digitized at 40x magnification using a digital video camera (Olympus DP71, Japan) mounted on a widefield microscope (Olympus BX53, Japan). The measurements were limited to cells that were round to ovoid with visible round nuclei, and 50 cells were counted in at least 10 images obtained from each left ventricle. CSA determinations were carried out using image analysis software (Image-Pro Plus v6.3 - Media Cybernetics, USA).

2.7. Collagen Determination in Left Ventricle

To assess collagen levels, the left ventricle sections were stained with the Picrosirius red technique (Direct Red 80, Aldrich, Milwaukee, WI 53233, USA). The samples were observed under polarized light using an analyzer (U-ANT, Olympus) and a polarizer (U-POT, Olympus) to analyze the birefringence of the stained collagen. Histological images were digitized at 20x magnification using a digital video camera (Olympus DP71, Japan)

mounted on a widefield microscope (Olympus BX53, Japan). The percentage of total collagen was calculated by summing the areas of all connective tissues (including type I and type III collagen) in the sections and dividing it by the total surface area of the section.

2.8. Sample preparation, electrophoresis and Western blot analysis

Homogenates were prepared from lysed ventricular tissue with RIPA buffer with protease and phosphatase inhibitors. After centrifugation, the supernatant was retained, and protein content was quantified using the Bradford method with bovine serum albumin as the standard. Proteins from cardiac homogenates (60 µg) were separated on SDS-polyacrylamide gels and transferred to PVDF membranes. The blots were then probed with antibodies raised against $p47^{phox}$ (sc-17845; Santa Cruz Biotechnology, 1:1.000), $gp91^{phox}$ (sc-130548; Santa Cruz Biotechnology, 1:1.000) SOD 1 (sc-17767; Santa Cruz Biotechnology, 1:1.000), Na^+/K^+ ATPase (ST0533, Thermofisher, 1:1.000) and GAPDH, glyceraldehyde 3-phosphate dehydrogenase, (sc-47724, Santa Cruz Biotechnology, 1:1.000). Peroxidase conjugated anti-rabbit (sc-2004; Santa Cruz Biotechnology, 1:10.000) or anti-mouse Ig-G H&L (ab 205719; Abcam, 1:10.000) were used as secondary antibodies. Immunoreactivity was visualized by a peroxidase-based chemiluminescence detection kit (Merck Millipore). The signal intensity of the bands in the immunoblots was quantified by densitometry using Image J software (NIH, USA).

2.9. Statistics

The data were expressed as means ± standard error of the mean (SEM). Group differences were evaluated using a one-way analysis of variance (ANOVA) with a Tuckey test for post hoc analysis. Two-way ANOVA with Bonferroni post hoc tests was employed to compare systolic blood pressure (SBP) values. Statistical significance was determined at a threshold of $P<0.05$. Data visualization and analysis were performed using GraphPad Prism 9.3.0 software.

3. Results

3.1. FTIR spectroscopy

The FTIR spectra of ZnMD and MD are shown in Fig. S2B. The vibrational modes of methyldopa and Zn-methyldopa were tentatively assigned by comparing them with reported data for L-dopa (Table 1) [31]. Due to the zwitterionic form of MD in the solid state, which results from the transfer of a proton from the carboxylic acid to the amino group, the FTIR spectrum of MD exhibited characteristic absorptions corresponding to the carboxylate and NH_3^+ groups. These included the COO^- stretch (asymmetric and symmetric), NH_3^+ stretch (very broad), and N-H bend (asymmetric and symmetric) bands. Therefore, the main bands in the vibrational spectrum of MD were assigned by comparing them with those of 5-OH tryptophan [32] and related aminoacids in their zwitterion form [33,34].

Table 1. Tentative assignments of the FTIR spectra of methyldopa and ZnMD (band postitions in cm^{-1}).

MD	ZnMD	Assignments
3473 vs	3508 sh	ν (OH)
3407 vs	3414 s	ν (N-H)
	3316 s	ν_{as} (NH_2)
	3256 s	ν_s (NH_2)
3218 vs	3160 s	
3100 m	--	ν_{as} (NH_3^+)
3046 m	--	ν_s (NH_3^+)
1647 sh, 1634 vs	1633 sh	ν(C=C) ring
1617 s	1584 vs	ν_{as} (COO^-)
1604 vs 1586 sh		δ (NH_3^+)
1533 m		δ (NH_2)
1492 s	1496 s	$\delta_{ip}C_{ring}OH$
1462 m	1462 m	δCOH, ν CO
1442 m	1419 m	ν_s (COO^-)
1402 s 1376 s	1403 m 1372 m	$\delta_{ip}CH_{ring}$, $\delta_{ip}C_{ring}OH$, δCCH
1346 m		δ (CH), ν (CC), ν(CN)
1330 m	1318 w	δ (CH), ν(CN)
1289 vs, 1257 s	1269 vs, br	δ CNH, $\delta_{ip}CH_{ring}$, $\nu C_{ring}O$
	1236 m	ν (C-OH)
1219 s		ν (C-OH) + ρ (NH_3^+)
1212 sh 1199 sh		ρ(NH_2)
1160 w 1126 m	1158 w 1128 m	ν (CC) + ν(CN) + ν (C-OH), phenol

s, strong; vs, very strong; w, weak; m, medium; sh, shoulder; v: stretching; δ: bending; ρ: rocking; ip: in-plane

The absence of C=O stretching band at 1657 cm^{-1} (which appears in the related compound L-dopa) indicates the zwitterionic form of MD. Bands associated with the carboxylate moiety in MD, such as ν_{as} (COO^-) and ν_s (COO^-) at 1617 cm^{-1} and 1442 cm^{-1}, respectively (Δ = 177 cm^{-1}) shifted to 1584 cm^{-1} and 1419 cm^{-1} (Δ = 165 cm^{-1}) upon metal interaction. The delta values suggested monodentate coordination of the carboxylate group. Direct comparisons of the N-H vibrational modes between MD and ZnMD were difficult to make, because of the protonation of this group in the ligand, and the deprotonation and metal coordination in the complex. However, the bands assigned to the stretching vibration involving C-NH for MD at 1289 cm^{-1} and 1247 cm^{-1}, merged in the metal complex showing a broad band centered at 1269 cm^{-1}, indicating Zn interaction with the amino group. Bands related to the OH (catechol) groups vibrations at 1492 cm^{-1}, 1462 cm^{-1}, 1402 cm^{-1}, 1376 cm^{-1} and 1158 cm^{-1}, 1128 cm^{-1} did not shift upon coordination, suggesting that these groups were not involved in the interaction with the metal center [35]. Furthermore, the absence of bands at approximately 1700 cm^{-1} (C=O stretching vibrations) indicates that oxidation of the catechol groups to quinone did not occur [36]. The modes below 1300 cm^{-1} are mainly due to combinations of bending vibrations within the molecule. Notwithstanding, the rocking mode of the NH_3^+ group can be assigned to the band located at 1219 cm^{-1} and is absent in the metal complex. The Zn-O stretching mode was located at 616 cm^{-1} [37]

3.2. NMR spectroscopy

The predicted spectrum of methyldopa is shown in Table 2 and Fig. S3. The ^1H NMR spectrum of the complex was recorded in DMSO-d6 and can be found in Table 2 and Fig. S4.

Table 2. ^{1}H NMR chemical shifts assignments (ppm) for methyl dopa (predicted and experimental spectra) and the ZnMD complex.

	MD predicted	MD experimental [38]	ZnMD
CH_3, Methyl group protons(singlet)	1.20	1.314	1.25
CH_2, Methylene protons	2.72	2.939; 2.698	1.94
HDO			3.49
NH_2, singlet	4.05		4.22
C, aromatic	6.51; 6.64; 6.68	6.505; 6.633; 6.722	6.53; 6.69; 6.70
OH, singlet	8.08		8.36
OH, singlet	8.91		8.84

The proton peaks in the ^{1}H NMR spectra of the ligand were assigned based on previous reports [39]. The experimental peaks corresponding to protons linked to oxygen and nitrogen atoms in the ligand may appear weak due to their exchange with the solvent protons.

In the Zn(II) complex, the aromatic signals do not exhibit significant shifts. However, the methyl and methylene proton resonances experience downfield shifts upon complexation with zinc. The predicted values in the ^{1}H NMR spectrum of methyldopa (Table 2) show some downfield shifts compared to the experimental peaks. Unfortunately, the experimental NH_2 resonance for the ligand could not be obtained, but it was observed at 4.22 ppm in ZnMD. It is expected that the NH_2 peak in MD would also undergo a downfield shift upon interaction with zinc [40]. The presence of peaks corresponding to hydroxyl groups in the complex indicates that there is no direct interaction between these groups and the metal center. This observation is consistent with the FTIR results, which suggest that the interaction of the metal with the ligand occurs primarily through the amino group. The interaction of the carboxylate moiety with

the metal center has also been determined through FTIR measurements. Fig. 2 showed the structure of the coordination complex obtained according to the physicochemical characterization.

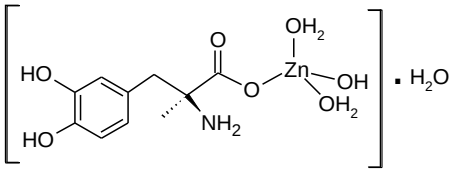

Fig. 2. Structure of $[ZnMD(OH)(H_2O)_2].H_2O$

3.3. Stability studies

To assess the stability of the complex during biological determinations, the changes in molar conductivity and electronic spectra over time were examined. Molar conductivity values were measured for a 1 x 10^{-3} M DMSO solution of ZnMD and were found to remain stable for 240 min, indicating that the complex remains stable in solution for at least 4 h (Table S1). The UV-vis spectra of ZnMD in DMSO also demonstrated that the complex remained stable throughout the experimental manipulations conducted for the biological measurements (Fig. S5).

3.4. In vitro BSA interactions

Human serum albumin (HSA) serves as the primary protein transporter in human blood plasma. However, in experimental investigations of drug-protein interactions, bovine serum albumin (BSA) is commonly used instead of HSA. This selection is due to the lower cost and greater availability of BSA, as well as the fact that the two proteins share a similar structure, despite minor differences in their amino acid sequences. Additionally, their binding characteristics are comparable. The albumin protein plays an important role as a drug carrier in the clinical applications. Its chemical structure and conformation enable interactions with a wide range of drugs, improving their pharmacokinetic properties [41]. Extensive research has been conducted on the specific binding of metal

complexes within the binding pockets of serum proteins [42]. It is well-established that the mammalian albumins, HSA and BSA allow the transport of pharmacologically active metal complexes [43]. In terms of antihypertensive treatment, the efficiency of the albumin-drug interactions is a critical factor affecting drug release and therapeutic effectiveness. Therefore, the study of the interaction between BSA and Zn complexes is crucial for understanding drug delivery. In previous works, we have determined that complexes formed between Zn and sartans exhibit a higher and reversible binding affinity to BSA compared to the commercial drugs. The enhanced binding may contribute to their increased antihypertensive effects [10,11,44,45]. Hence, the studying the binding of BSA to ZnMD will help to determine if the compound can be effectively distributed in the plasma, thus facilitating its pharmacological effect.

To examine the interactions between compounds and BSA, including the mechanism, binding constants, and number of binding sites, fluorescence quenching measurements (the decrease in fluorescence intensity of the fluorophore) were conducted [46]. BSA exhibits intrinsic fluorescence with a prominent emission peak at 336 nm when excited at 280 nm, primarily attributed to the excitation of the tryptophan group. However, upon titrating BSA with increasing concentrations of MD and ZnMD, the emission intensity of this peak notably decreased, indicating significant quenching of the fluorophore residues within BSA.

The fluorescence intensities measured with, (F), or without the quencher (F_0), at different concentrations [Q], allow for the determination of the Stern-Volmer quenching constant, K_{SV}, using the Stern-Volmer equation: $F_0/F = 1 + K_q\tau_0[Q] = 1 + K_{SV}[Q]$ (where τ_0 represents the lifetime of the fluorophore in the absence of the quencher and is considered as 1×10^{-8} s for a biopolymer) [46]. Fig. 3 shows the graphs obtained at different temperatures for MD and ZnMD. The quenching processes can be classified as static or dynamic. Dynamic quenching is characterized by an increase in K_{SV} with rising temperature, whereas static quenching is associated with a decrease in the Stern-Volmer constant. The observed results indicate that a static interaction occurs upon the

binding of the compounds to the protein. Furthermore, considering that the scattering collision quenching of various quenchers with biopolymers is typically around 2.0 x 10^{10} L mol^{-1} s^{-1}, the K_q values presented in Table 3 also support the conclusion that the compounds bind to the protein through static quenching.

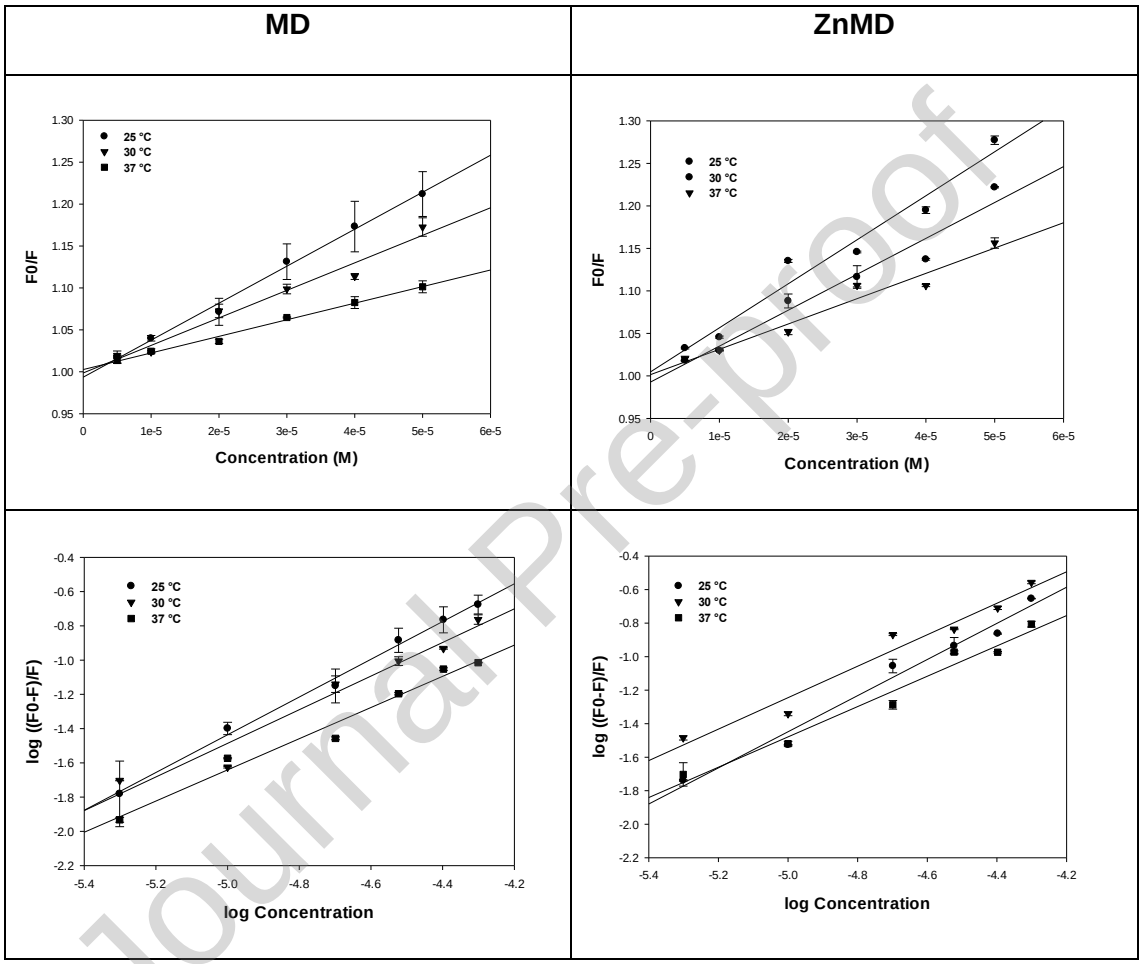

Fig. 3. Plots of F_0/F vs [Q] and log [(F_0 - F)/F] vs. log [Q] for the interaction of BSA with α-Methyldopa (MD) and [ZnMD(OH)(H_2O)$_2$].H_2O (ZnMD), at different temperatures. [BSA] = 6 μM, λ_{ex} = 280 nm.

Table 3. Stern–Volmer constant (Ksv), bimolecular quenching constant (Kq), binding constant (Ka) and number of binding sites (n) for the interaction of α-Methyldopa (MD) and $[ZnMD(OH)(H_2O)_2].H_2O$ (ZnMD), with BSA (6 μM) in Tris-HCl buffer (0.1 M, pH 7.4).

	MD						ZnMD					
T (°C)	25		30		37		25		30		37	
1/T (10^{-3}) (1/K)	3.354		3.299		3.224		3.354		3.299		3.224	
log K_a ± SD	4.074	±	3.422	±	2.911	±	3.941	±	3.448	±	3.046	±
	0.192		0.169		0.132		0.185		0.166		0.127	
n ± SD	1.102	±	0.982	±	0.910	±	1.078	±	0.939	±	0.905	±
	0.042		0.036		0.029		0.039		0.044		0.044	
K_a (10^3) ± SD	11.857	±	2.642	±	0.814	±	8.729	±	2.805	±	1.111	±
($Lmol^{-1}$)	0.524		0.111		0.037		0.314		0.104		0.051	
K_q (10^{12})	4.413	±	3.283	±	1.979	±	4.225	±	5.180	±	2.978	±
($M^{-1}s^{-1}$)	0.195		0.163		0.089		0.178		0.239		0.131	
K_{sv} (10^3) ± SD	4.413	±	3.283	±	1.979	±	4.225	±	5.180	±	2.978	±
($Lmol^{-1}$)	0.195		0.163		0.089		0.178		0.239		0.131	

Using the Scatchard equation: $\log[(F_0 - F)/F] = \log K_a + n \log[Q]$, for a static quenching, the binding constants (K_a) and the number of binding sites (n) were determined, as shown in Fig. 3 and Table 3. The stability constants decrease with increasing temperature, which is consistent with the decrease in stability of the BSA-compound complexes. The number of binding sites, n approximately 1, is an indication that the compounds interacted with only one binding site of BSA. The values of K_a can provide insights into the toxicity, biological activity, and pharmacokinetic properties of a drug, as they reflect the fraction of drugs bound to proteins in the blood. Considering albumin as the main protein carrier for drugs in the bloodstream, the binding data are correlated with the transport and disposition of a compound and it has been suggested that an efficient interaction with the protein occurs for K_a values between 10^3 and 10^6 $L.mol^{-1}$. The obtained binding constants for MD and ZnMD, suggest a moderate affinity of the compounds for BSA, indicating that they can be stored, transported, and eliminated from the protein.

During the interaction between BSA and the compounds, various binding forces can occur. To determine the nature of these binding forces, the thermodynamic parameters,

namely entropy (ΔS), enthalpy (ΔH), and Gibbs free energy (ΔG), were calculated using the van't Hoff equation: ln K_a = -ΔH/RT + ΔS/R (where R = 0.008314 kJ/Kmol is the gas constant; see Fig. 4). The negative values of ΔG obtained at three different temperatures (Table 4), as determined by the equation ΔG = ΔH - TΔS, indicate a spontaneous binding of the compounds to BSA [47].

The binding forces can be divided into hydrogen bonding, hydrophobic interaction, van der Waals forces and electrostatic interactions [48], based on the signs of the entropy and enthalpy changes. The enthalpy and entropy changes were found to be negative, suggesting that the interaction between the compounds and BSA is primarily driven by hydrogen bonding and van der Waals force [48]. Both compounds display similar free energy changes according to the similar K_a values calculated at each temperature (ΔG = - 0.008314 T ln K_a, kJ/Kmol). Notwithstanding, they showed different negative enthalpy and entropy changes.

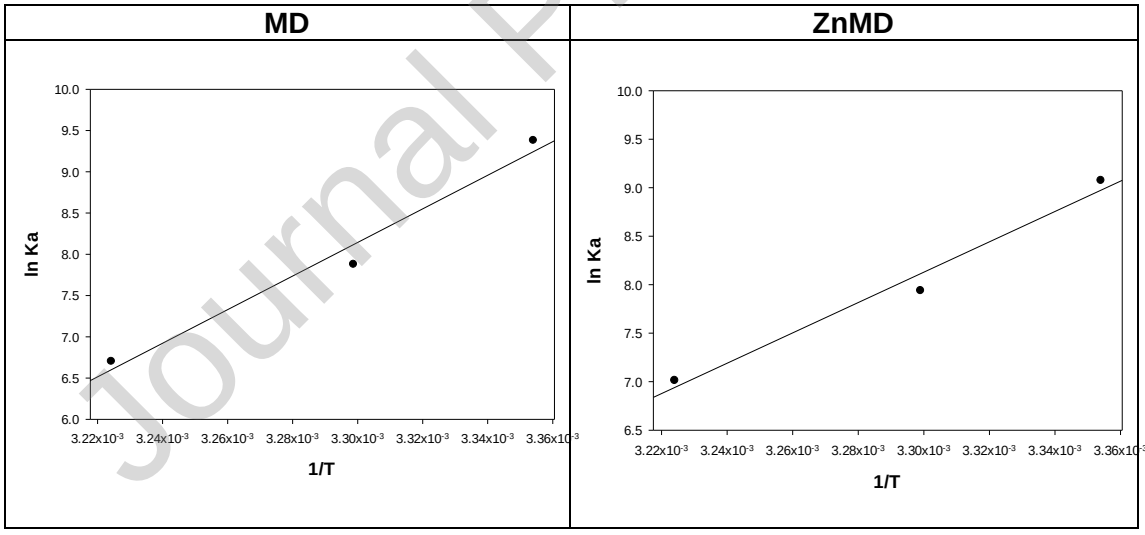

Fig. 4. Plot of lnK_a vs. 1/T for calculation of the thermodynamic parameters for MD and ZnMD.

Table 4. Thermodynamic parameters for α-Methyldopa (MD) and $[ZnMD(OH)(H_2O)_2].H_2O$ (ZnMD)

	MD			ZnMD		
T (°C)	25	30	37	25	30	37
1/T (10^{-3}) (1/K)	3.354	3.299	3.224	3.354	3.299	3.224
ΔS (KJ/mol)	-0.491 ± 0.023			-0.362 ± 0.017		
ΔH (KJ/mol)	-169.31 ± 8.322			-130.81 ± 6.472		
ΔG (KJ/mol)	-22.92	-20.46	-17.02	-22.25	-20.44	-17.91

3.5. In vivo studies

3.5.1. Effect of ZnMD in the SBP in SHRs

At the begging of the experiment, the systolic blood pressure (SBP) values of SHR groups ranged between 189 and 210 mmHg. During the treatment period, the untreated group maintained stable blood pressure. After eight weeks of treatment, both MD and ZnMD diminished the SBP being ZnMD statistically different from MD alone. Animals treated with Zinc did not show changes in SBP. (Fig. 5).

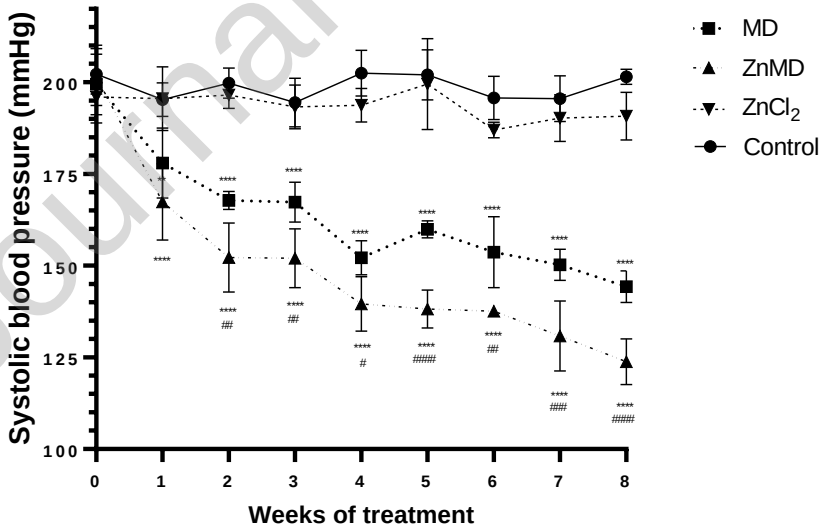

Fig. 5. Time course of systolic blood pressure (SBP), measured by tail-cuff plethysmography, in spontaneously hypertensive rats (SHR) treated with MD, ZnMD and $ZnCl_2$. Values are means ± SEM (n=4-5). (*) Statistically different values between MD,

ZnMD and control (***p<0.001; ****p<0.0001), (#) Statistically different values between MD or ZnMD at the same concentration (#p<0.05. ###; p>0.001)

3.6. Ex Vivo Assays

3.6.1. Effects of ZnMD on Cardiac hypertrophy, function and fibrosis in SHRs

SHR rats were echocardiographycally monitoreated to assess the extent of heart hypertrophy. The measurements included posterior wall thickness in diastole (PWd) and the left ventricular mass index (LVMI) that was derived using the LV mass/tibial length ratio. In addition, the percentage of fractional shortening (%) at the end of treatment was calculated.

The ZnMD treatment, in conjunction with the reduction of arterial pressure, resulted in a decrease in myocardial hypertrophy as indicated by lower LVMI and reduced ΔPWd. This reduction in myocardial hypertrophy was accompanied by a decrease in cardiomyocyte cross-sectional area CSA (Fig. 6 Fig. S6). Moreover, ZnMD treatment improved heart function, as evidenced by the fractional shortening (FS, %). In contrast, the MD intervention alone did not show noticeable differences in these parameters. Consistent with these results, previous studies by other authors did not demonstrate significant changes in LVMI, PW and ejection fraction with MD treatment [49]. These findings suggest that higher doses of MD (ranging from 500 to 750 mg/day) and a longer duration of therapy may be required to reverse heart hypertrophy. [50,51].

To further investigate the cardioprotective effects of ZnMD treatment, the Picrosirius red staining revealed a significant reduction in collagen type I and an increment of collagen type III, indicating a decrease in myocardial stiffness. In contrast, MD treatment failed to attenuate the left ventricular fibrosis (Fig. 6 Fig. S7).

Then, we observed an improvement in cardiovascular function and geometry in the animals treated with ZnMD, but not with MD alone, suggesting that this parameter is dependent on variables other than the hemodynamic effects. Animals treated with Zinc showed no changes in either morphology or cardiac function.

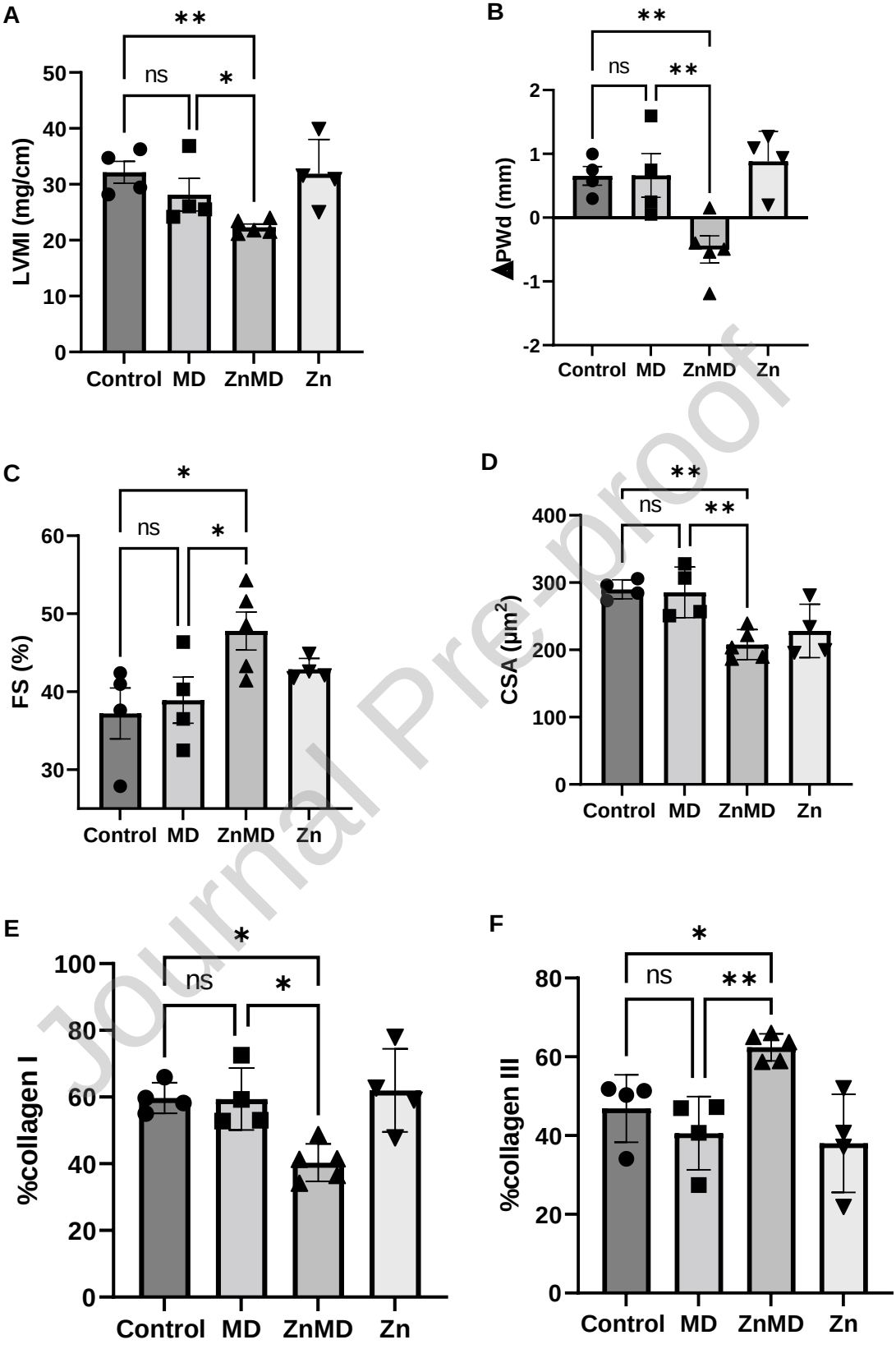

Fig. 6. Evaluation of cardiac hypertrophy and function by echocardiography and fibrosis assessment of SHR treated with MD, ZnMD and Zn. A: left ventricular mass index (LVMI), B: posterior wall thickness in diastole (ΔPWd), C: percentage of fractional shortening (FS%), D: Cross sectional area (CSA) of left ventricular cardiomyocytes. E, F: percentage of collagen type I and III. Values are means ± SEM (n=4-5). (*) Statistically different values between MD, ZnMD and control (*p<0.05; **p<0.01; ***p<0.001; ****p<0.0001)

3.6.2. Effects of ZnMD on Oxidative stress

Oxidative stress can lead to several cardiac alterations, including mitochondrial dysfunction, where reactive oxygen species (ROS) disrupt the respiratory chain and activate multiple protein kinases and transcription factors involved in hypertrophic signaling[52]. To assess the potential contribution of ZnMD to prevent oxidative stress, biomarkers related to cardiac redox status were determined. As shown in Fig. 7, ZnMD significantly reduced ROS production in comparison with non-treated and Zinc groups and decreased the lipid peroxidation, as a parameter of the damage generated by ROS. It was demonstrated that plasma samples from patients with gestational arterial hypertension treated with different concentrations of MD did not show significant differences compared to untreated patients in terms of TBARS levels [53], or did not exhibit any antioxidant effect in peripheral blood [54]. In line with such reports, our results showed that in the MD group, oxidative damage was not ameliorated.

To investigate whether ZnMD and MD regulate cardiac NADPH oxidase (NOX2), the major source of ROS, or in SOD1 expression, an antioxidant enzyme, the expression of the catalytic subunit $gp91^{phox}$, the cytoplasmic subunit $p47^{phox}$ and the enzyme SOD1 were assessed using western blot analysis. The results showed that the ZnMD complex exerted an inhibitory effect on $gp91^{phox}$ and $p47^{phox}$ expression while increasing SOD levels. In contrast, the parental drug MD did not show any significant effect on SOD expression, which is consistent with previous reports [54]. However, its reduction on

gp91^{phox} and p47^{phox} subunit expression is not fully understood and warrants further investigation, possibly it is not enough to reduce ROS production and its consequent damage. Taken together, the data indicate that ZnMD treatment improves redox signaling by reducing left ventricular ROS generation, associated with a decrease in the expression of the NAD(P)H oxidase subunits gp91^{phox} and p47^{phox}, and an increment in the scavenger system SOD 1.

Nitric oxide (NO) is produced by cardiac myocytes and acts as a potent vasodilator, exerting a relaxing effect on the myocardium [55]. NO is generated in the heart by three Nitric Oxide Synthase isoforms (NOS) and any dysfunction in these enzymes can lead to reduce NO production and result in hypertrophy [56]. Excessive ROS can bind to NO, affecting its bioavailability and causing cardiac and endothelial dysfunction as well as hypertension [57]. To investigate whether the effects of ZnMD on cardiac function were related to changes in NO, its levels were measured. Interestingly, SHRs treated with MD showed increased NO production compared to non-treated rats, but the levels of NO were even higher in the presence of ZnMD treatment (Fig. 7). These results indicate that the increase in NO levels accompanied by a decrease in ROS, observed with ZnMD treatment, may be involved in the antihypertrophic effects of ZnMD. Overall, these findings suggest that ZnMD treatment may promote a favorable balance between NO and ROS levels, which could contribute to the observed antihypertrophic effects and improved cardiac function in the treated rats.

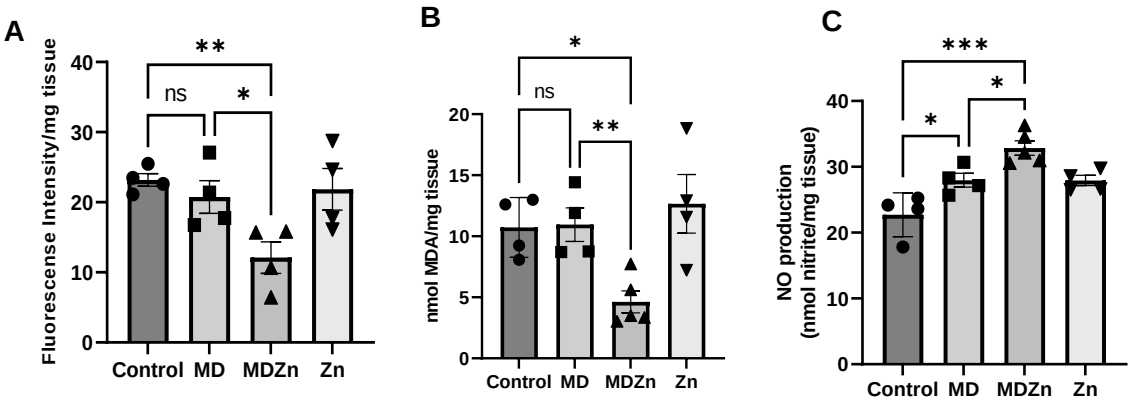

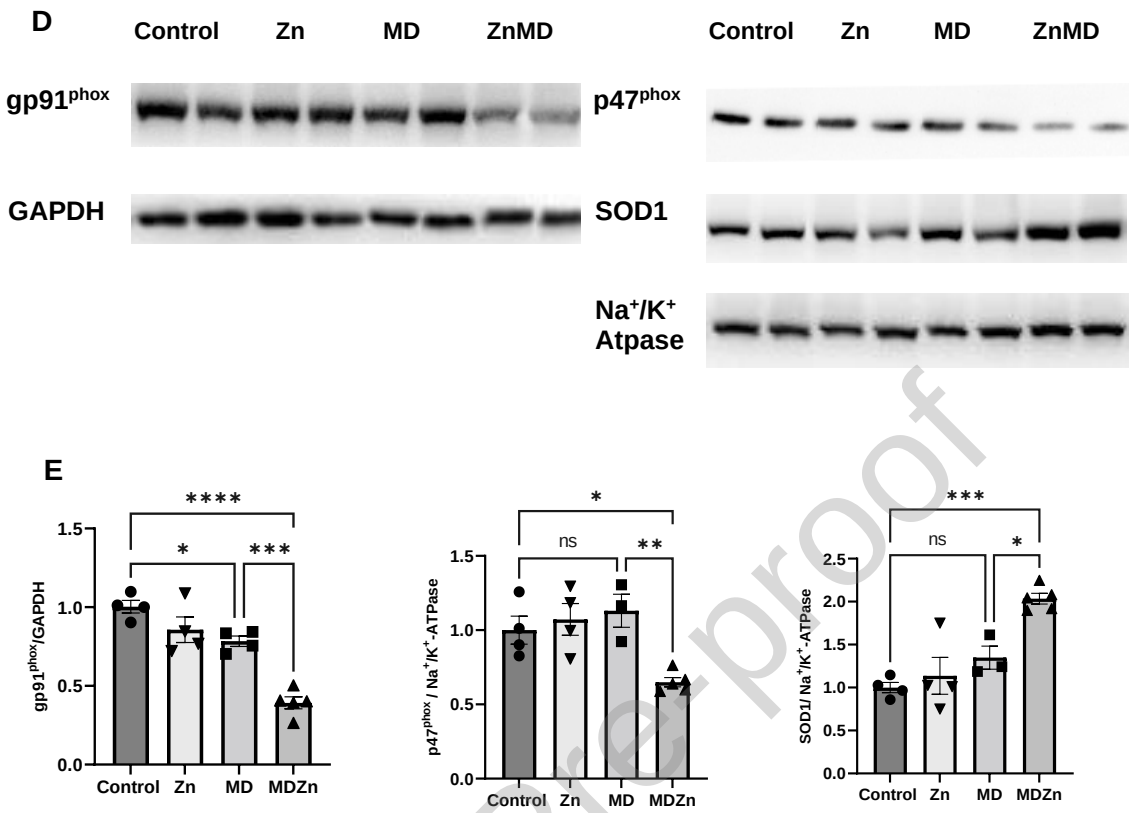

Fig. 7. Oxidative stress evaluation on hearts obtained from SHR treated with MD, ZnMD and Zn. A: ROS production B: TBARS assay C: NO levels D, E: Representative bands and plots of western blot of $gp91^{phox}$ and $p47^{phox}$ subunits and SOD1 expression. E: Data are expressed as mean ± SEM. Statistically significant differences are represented by: *p<0.05; **p<0.01; ***p<0.001; ****p<0.0001

4. Discussion

A new Zn complex with the antihypertensive drug α-methyldopa has been synthesized and characterized by FTIR, NMR and UV-Vis spectroscopies, elemental analysis and thermogravimetric and conductance determinations. The interaction between the ligand and the Zn complex with BSA is characterized as a spontaneous and reversible binding process, exhibiting similar K_a constants. By determining the thermodynamic parameters, it is suggested that the binding process is driven by enthalpy, involving the formation of

Van der Waals forces and hydrogen bonds. Therefore, it can be concluded that the complex has the potential to be transported reversibly by albumin.

The reduction of blood pressure and the lowering of left ventricular weight after a long-term administration of MD to spontaneously hypertensive rats was previously reported [51]. α_2-adrenergic receptors are part of the G protein-coupled receptors family and function as feedback inhibitors of norepinephrine release in adrenergic neurons [58]. They play a significant role in regulating blood flow by inducing constriction/vasorelaxation in the smooth muscle wall of major arteries, thereby influencing cardiac physiology. These receptors are expressed in the cardiac presynaptic sympathetic nerve terminal, as well as in the kidney, vasculature and heart. Dysfunction of these receptors can lead to increased cardiac norepinephrine release or adrenal medulla secretion, resulting in elevated arterial tension, oxidative stress, and cardiomyocyte hypertrophy in the left ventricular tissue [59–61]. Various agonist drugs, such as α-methyldopa, clonidine, brimonidine, and moxonidine, can activate these receptors, thus preventing hypertension, cardiac hypertrophy, and fibrosis. Their activation helps to regulate blood pressure and protect against adverse cardiac remodeling [62,63]. In summary, α_2-adrenergic receptors have a crucial role in maintaining cardiovascular homeostasis, and their proper activation by specific drugs can be beneficial in preventing cardiac complications associated with hypertension and hypertrophy.

Stimulation of the α-adrenergic nervous system leads to increased protein synthesis, expression of hypertrophic markers, and enlargement of cardiac muscle cells [64,65], contributing to cardiac remodeling as a compensatory mechanism in response to wall stress, hemodynamic pressure, or volumetric burden. However, this pathological hypertrophy can be detrimental to heart function [2]. It has been found that better agonism of the cardiac and vascular pre-synaptic α_2-adrenergic receptor can restore blood pressure to the normal range, regress the cardiac hypertrophy and mitigate the damage [61,66]. In this study, the antihypertensive effect observed by ZnMD in SHRs

was stronger than that achieved with MD treatment alone. Interestingly, this hypotensive action of the MD did not result in a reduction of cardiac hypertrophy, fibrosis, or oxidative stress. These findings suggest that ZnMD could exhibit a stronger binding affinity to the α_2-adrenergic receptor compared to MD. One possible explanation for this probable enhanced interaction is that the binding of the agonist to α_2-adrenergic receptors involves π-π or cation-π interactions through a Phe residue (F7.39) that acts as a lid in agonist bound structure [67]. The presence of the cation zinc in the complex may result in enhanced binding to the receptor pocket. Furthermore, the F7.39 is conserved in α_1-adrenergic receptors, and studies have shown that the interaction of zinc with this receptor acts as a positive allosteric modulator, enhancing the agonism of the neurotransmitter [68]. Additionally, and according the findings of Chen *et al.* on the α_2-adrenergic receptor activation, it can been suggested that the hydroxyl groups and water molecules of ZnMD may form hydrogen bonds with the transmembrane domain 5 (TM5) causing a modification of the loosened helix structure of TM4 and inducing a change in the second extracellular loop, which is directly involved in ligand binding and activation of α_2-adrenergic receptor [69]. These interactions may explain the superior effects of ZnMD compared to MD in reducing blood pressure and ameliorating cardiac hypertrophy and oxidative stress.

The observed antihypertensive and antihypertrophic effects of ZnMD can be attributed to its ability to decrease cardiac ROS production by reducing the expression of NAD(P)H oxidase subunits ($gp91^{phox}$ and $p47^{phox}$) and increasing SOD1 expression in the left ventricle. As a result, there is an increase in NO bioactivity and an improvement in heart function. Elevated concentrations of catecholamines, which can occur in hypertension, can induce oxidative mechanisms by activating NAD(P)H oxidase, leading to worsened myocardial hypertrophy and fibrosis [70]. Moreover, norepinephrine downregulates NO levels in cardiomyocytes [71] further contributing to cardiac dysfunction. The beneficial effects of ZnMD may involve its effective interaction with the α_2-adrenergic receptor, enhancing agonism and increasing negative feedback to reduce norepinephrine release.

By restoring the redox status, ZnMD increases NO availability, which improves cardiac function (as evidenced by %FS) [57].

The excessive intake of Zn increased blood pressure and reduced renal function through the increase of oxidative stress. A previous report working with Male Sprague-Dawley rats weighing 180-210 g, shows that a control diet contains 1.1 mg Zn/d and excess diets contain 11 mg Zn/d and 44 mg Zn/d [72]. In our experiments we worked with Male spontaneously hypertensive rats (SHRs) weighing 200-300 g. They received $ZnCl_2$ (64.5 mg/kg/d) or Zn (30.9 mg/kg/d), an average of 7.7 mg Zn/d, below the 11 mg Zn/d of the excess, and this quantity did not affect BP and ROS generation.

In summary, the results of this study have revealed a connection between the adrenergic agonism and hypertrophic signaling in heart. We propose that ZnMD significantly reduces blood pressure by potentially enhancing its binding to the adrenergic receptor in the postsynaptic neuron. This enhanced binding may prevent the release of norepinephrine, a neurotransmitter implicated in vasoconstriction. Consequently, lower levels of norepinephrine may promote vasodilation. Additionally, due to its increased effectiveness, ZnMD requires lower doses to achieve antihypertensive effects compared to previously reported MD treatments. These earlier treatments necessitate doses twenty to forty times higher, which can lead to adverse effects on the central nervous system. [73–75].

The demonstrated antihypertensive effects of ZnMD also exert a direct infuence on the cardiac structure. They reduce the chronic workload on the heart, resulting in a reduction in left ventricular mass. Additionally, by inhibiting the release of norepinephrine, ZnMD reduces ROS generation through cardiac NAD(P)H oxidase activity, mechanism accompanied by an increase of SOD1 expression. This reduction in ROS levels is associated with a decrease in fibrosis, resulting in improved cardiac elasticity and enhanced cardiac function. Furthermore, ZnMD promotes the production of nitric oxide (NO), which contributes to cardiac relaxation and vasodilation. These findings provide important evidence suggesting that this complex could be a potential therapeutic drug

for the treatment of hypertension, cardiac hypertrophy, and dysfunction. The novel properties of ZnMD make it a promising candidate for further investigation as a potential treatment option in cardiovascular diseases.

5. Conclusions

The new metal complex formed with the essential element Zn and the antihypertensive drug α-methyldopa, ZnMD, improved the biological properties of the parent drug. ZnMD treatment have a protective effect against oxidative stress in the heart, while MD alone may not provide the same level of protection. These findings suggest that the treatment with the structural modified drug by Zn complexation, may play a role in modulating the expression of key proteins involved in ROS generation and scavenging, potentially contributing to the observed reduction in ROS levels and cardiac redox status. The specific mechanisms underlying the differential effects of ZnMD and MD on NOX2 and SOD1 expression require further exploration. It is possible that the ZnMD treatment may lead to different mechanisms of action or synergistic effects, contributing to the observed cardioprotective effects. Overall, these findings suggest that ZnMD treatment may promote a favorable balance between NO and ROS levels, which could contribute to the observed antihypertrophic and antifibrotic effects accompanied by an improvement in cardiac function in the treated rats.

Supplementary Information. **Fig. S1.** Thermogravimetric analysis of $[ZnMD(OH)(H_2O)_2].H_2O$. Oxygen flow of 50 mL min^{-1}; heating rate 10 °C min^{-1}. **Fig. S2.** **Figure S2.** A. FTIR spectrum of the residue of the TGA measurement. B. FTIR spectra of methyldopa and ZnMD in KBr. Assignments for ZnMD. **Fig. S3.** Predicted ^1H NMR spectrum of methyldopa. **Fig. S4.** ^1H NMR spectrum of the complex of $[ZnMD(OH)(H_2O)_2].H_2O$ recorded in DMSO-d6. **Fig. S5.** Spectral variation of 1 x 10^{-4} M DMSO-ZnMD solution with time. **Fig. S6.** Representative microphotographs showing cross-sectional area (CSA) of cardiomyocytes. Magnification, 20. Bar indicates 10 μm.

Fig. S7. Representative Picrosirius red staining images, type I collagen fibers appear bright and red-yellow in comparison to type III collagen, which appears green. **Table S1**. Molar conductivity of ZnMD in DMSO during 240 min.

Acknowledgements The authors thank to Leandro Di Cianni for the technical support to measure the blood pressure and Dr. Nadir Jori, for the measurements of the RMN spectrum.

Author Contribution Agustin Actis Dato: conceptualization, methodology, software, data curation. Valeria R. Martinez: methodology, data curation, writing-original draft review and editing. Jorge O. Velez Rueda: methodology and data curation. Enrique L. Portiansky: conceptualization, methodology, writing-review and editing. Verónica De Giusti; methodology writing-review and editing. Evelina G. Ferrer: conceptualization, methodology, writing-review and editing. Patricia A.M Williams: conceptualization, methodology, writing original draft-review and editing, supervision.

Funding This work was supported by: UNLP [X/871, V720], CONICET [PIP 1999], CICPBA and ANPCyT [PICT-2019-0945] Argentina. AAD and VRM are fellowship holders of CONICET. ELP, VDG, and EGF are research fellows of CONICET and PAMW is research fellow of CICPBA.

Data Availability The datasets generated during the current study are available from the corresponding author on reasonable request.

Declaration of Competing Interests The authors declare no competing interests.

References

[1] World Health Organization, Hypertension, (2023). https://www.who.int/news-room/fact-sheets/detail/hypertension (accessed July 30, 2023).

[2] S. Saheera, P. Krishnamurthy, Cardiovascular Changes Associated with Hypertensive Heart Disease and Aging, Cell Transplant. 29 (2020) 096368972092083. https://doi.org/10.1177/0963689720920830.

[3] M. Seddon, Y.H. Looi, A.M. Shah, Oxidative stress and redox signalling in cardiac hypertrophy and heart failure, Heart. 93 (2007) 903–907. https://doi.org/10.1136/hrt.2005.068270.

[4] K. Holland, Everything You Need to Know About High Blood Pressure (Hypertension), (2023). https://www.healthline.com/health/high-blood-pressure-hypertension#definition (accessed July 30, 2023).

[5] T.M. Brody, J. Larner, K.P. Minneman, Human Pharmacology: Molecular to Clinical, in: Human Pharmacology: Molecular to Clinical, 1998.

[6] M. HENNING, A. RUBENSON, Evidence that the hypotensive action of methyldopa is mediated by central actions of methylnoradrenaline, Journal of Pharmacy and Pharmacology. 23 (1971). https://doi.org/10.1111/j.2042-7158.1971.tb08671.x.

[7] M. Fouladgar, S. Ahmadzadeh, Application of a nanostructured sensor based on NiO nanoparticles modified carbon paste electrode for determination of methyldopa in the presence of folic acid, Appl Surf Sci. 379 (2016). https://doi.org/10.1016/j.apsusc.2016.04.026.

[8] D. van de Vusse, P. Mian, S. Schoenmakers, R.B. Flint, W. Visser, K. Allegaert, J. Versmissen, Pharmacokinetics of the most commonly used antihypertensive drugs throughout pregnancy methyldopa, labetalol, and nifedipine: a systematic review, Eur J Clin Pharmacol. 78 (2022). https://doi.org/10.1007/s00228-022-03382-3.

[9] P.A.M. Williams, Metal complexes of the antihypertensive drugs that inhibit the renin-angiotensin system, Curr Trends Med Chem. 7 (2014) 97–104.

[10] V.R. Martínez, M. V Aguirre, J.S. Todaro, A.M. Lima, N. Stergiopulos, E.G. Ferrer, P.A. Williams, Zinc complexation improves angiotensin II receptor type 1 blockade and *in vivo* antihypertensive activity of telmisartan, Future Med Chem. 13 (2021) 13–23. https://doi.org/10.4155/fmc-2020-0093.

[11] V.R. Martinez, A. Martins Lima, N. Stergiopulos, J.O. Velez Rueda, M.S. Islas, M. Griera, L. Calleros, M. Rodriguez Puyol, C. Jaquenod de Giusti, E.L. Portiansky, E.G. Ferrer, V. De Giusti, P.A.M. Williams, Effect of the structural modification of Candesartan with Zinc on hypertension and left ventricular hypertrophy, Eur J Pharmacol. 946 (2023) 175654. https://doi.org/10.1016/j.ejphar.2023.175654.

[12] A.G. Restrepo Guerrero, V.R. Martinez, J.O. Velez Rueda, E.L. Portiansky, V. De Giusti, E.G. Ferrer, P.A.M. Williams, Complexation of the Antihypertensive Drug Olmesartan with Zn: In Vivo Antihypertensive and Cardiac Effects, Biol Trace Elem Res. (2023). https://doi.org/10.1007/s12011-023-03670-8.

[13] B.L. Vallee, K.H. Falchuk, The biochemical basis of zinc physiology., Physiol Rev. 73 (1993) 79–118. https://doi.org/10.1152/physrev.1993.73.1.79.

[14] Q. Zhang, Y. Xue, Y. Fu, B. Bao, M. Guo, Zinc Deficiency Aggravates Oxidative Stress Leading to Inflammation and Fibrosis in Lung of Mice, Biol Trace Elem Res. 200 (2022) 4045–4057. https://doi.org/10.1007/s12011-021-03011-7.

[15] J. Lu, A.J. Stewart, D. Sleep, P.J. Sadler, T.J.T. Pinheiro, C.A. Blindauer, A molecular mechanism for modulating plasma Zn speciation by fatty acids, J Am Chem Soc. 134 (2012). https://doi.org/10.1021/ja210496n.

[16] G.V. Fazakerley, P.W. Linder, R.G. Torrington, M.R.W. Wright, Potentiometric and spectrophotometric studies of the copper(II) complexes of methyldopa, methyltyrosine, and catechol in aqueous solution, Journal of the Chemical Society, Dalton Transactions. (1979) 1872. https://doi.org/10.1039/dt9790001872.

[17] G.D. Peckham, I.J. McNaught, A.T. Hutton, Thermodynamic studies on metal-ligand complexes: Copper(II) complexes of alanine, phenylalanine and catechol, South African Journal of Chemistry. 51 (1998).

[18] H.L. Slates, D. Taub, C.H. Kuo, N.L. Wendler, Degradation of α-Methyl-3,4-dihydroxyphenylalanine (α-MethylDOPA), J Org Chem. 29 (1964) 1424–1429. https://doi.org/10.1021/jo01029a039.

[19] K.S. Rajan, A.A. Manian, J.M. Davis, H. Dekirmenjian, Metal chelates of l-DOPA for improved replenishment of dopaminergic pools, Brain Res. 107 (1976) 317–331. https://doi.org/10.1016/0006-8993(76)90229-8.

[20] B. Kalyanaraman, R.C. Sealy, Electron spin resonance-spin stabilization in enzymatic systems: Detection of semiquinones produced during peroxidatic oxidation of catechols and catecholamines, Biochem Biophys Res Commun. 106 (1982) 1119–1125. https://doi.org/10.1016/0006-291X(82)91228-1.

[21] C.E. Säbel, J.M. Neureuther, S. Siemann, A spectrophotometric method for the determination of zinc, copper, and cobalt ions in metalloproteins using Zincon, Anal Biochem. 397 (2010) 218–226. https://doi.org/10.1016/j.ab.2009.10.037.

[22] S. Sood, A. Kumar, N. Sharma, Photocatalytic and Antibacterial Activity Studies of ZnO Nanoparticles Synthesized by Thermal Decomposition of Mechanochemically Processed Oxalate Precursor, ChemistrySelect. 1 (2016). https://doi.org/10.1002/slct.201601435.

[23] J. Li, B.A. Kemp, N.L. Howell, J. Massey, K. Mińczuk, Q. Huang, M.D. Chordia, R.J. Roy, J.T. Patrie, G.E. Davogustto, C.M. Kramer, F.H. Epstein, R.M. Carey, H. Taegtmeyer, S.R. Keller, B.K. Kundu, Metabolic Changes in Spontaneously

Hypertensive Rat Hearts Precede Cardiac Dysfunction and Left Ventricular Hypertrophy, J Am Heart Assoc. 8 (2019). https://doi.org/10.1161/JAHA.118.010926.

[24] J. Charan, N.D. Kantharia, How to calculate sample size in animal studies?, J Pharmacol Pharmacother. 4 (2013) 303–306. https://doi.org/10.4103/0976-500X.119726.

[25] M.R. Warren, A. Radulescu, P. Dornbos, D. Cuomo, S. Zumwalt, D. Bueso-Mendoza, M. Nitcher, J.J. LaPres, D.W. Threadgill, Peanut butter as an alternative dose delivery method to prevent strain-dependent orogastric gavage-induced stress in mouse teratogenicity studies, J Pharmacol Toxicol Methods. 107 (2021) 106948. https://doi.org/10.1016/j.vascn.2020.106948.

[26] P. Chatelain, M. Waelbroeck, J.-C. Camus, P. de Neef, P. Robberecht, J. Roba, J. Christophe, Comparative effects of α-methyldopa, propranolol and hydralazine therapy on cardiac adenylate cyclase activity in normal and spontaneously hypertensive rats, Eur J Pharmacol. 72 (1981) 17–25. https://doi.org/10.1016/0014-2999(81)90292-2.

[27] E.F. Jones, S.B. Harrap, P. Calafiore, A.M. Tonkin, Development and validation of echocardiography methods for estimating left ventricular mass in rats, Clin Exp Pharmacol Physiol. 19 (1992) 361–364. https://doi.org/10.1111/j.1440-1681.1992.tb00472.x.

[28] R.B. Devereux, N. Reichek, Echocardiographic determination of left ventricular mass in man. Anatomic validation of the method., Circulation. 55 (1977) 613–618. https://doi.org/10.1161/01.CIR.55.4.613.

[29] H. Ohkawa, N. Ohishi, K. Yagi, Assay for lipid peroxides in animal tissues by thiobarbituric acid reaction, Anal Biochem. 95 (1979) 351–358. https://doi.org/10.1016/0003-2697(79)90738-3.

[30] O. Mizuno, S. Kobayashi, K. Hirano, J. Nishimura, C. Kubo, H. Kanaide, Stimulus-specific alteration of the relationship between cytosolic Ca^{2+} transients and nitric oxide production in endothelial cells *ex vivo*, Br J Pharmacol. 130 (2000) 1140–1146. https://doi.org/10.1038/sj.bjp.0703420.

[31] B. Edwin, I. Hubert Joe, Vibrational spectral analysis of anti-neurodegenerative drug Levodopa: A DFT study, J Mol Struct. 1034 (2013) 119–127. https://doi.org/10.1016/j.molstruc.2012.09.004.

[32] J.J. Martínez Medina, L.G. Naso, A.L. Pérez, A. Rizzi, N.B. Okulik, M. Valcarcel, C. Salado, E.G. Ferrer, P.A.M. Williams, Synthesis, characterization, theoretical studies and biological (antioxidant, anticancer, toxicity and neuroprotective) determinations of a copper(II) complex with 5-hydroxytryptophan, Biomedicine and Pharmacotherapy. 111 (2019) 414–426. https://doi.org/10.1016/j.biopha.2018.12.098.

[33] B.Z. Chowdhry, T.J. Dines, S. Jabeen, R. Withnall, Vibrational Spectra of α-Amino Acids in the Zwitterionic State in Aqueous Solution and the Solid State:

DFT Calculations and the Influence of Hydrogen Bonding, J Phys Chem A. 112 (2008) 10333–10347. https://doi.org/10.1021/jp8037945.

[34] K. Sharma, S.P. Sharma, S.C. Lahiri, Spectrophotometric, Fourier transform infrared spectroscopic and theoretical studies of the charge–transfer complexes between methyldopa [(S)-2 amino-3-(3,4-dihydroxyphenyl)-2-methyl propanoic acid] and the acceptors (chloranilic acid, o-chloranil and dichlorodicyanobenzoquinone) in acetonitrile and their thermodynamic properties, Spectrochim Acta A Mol Biomol Spectrosc. 92 (2012) 212–224. https://doi.org/10.1016/j.saa.2012.02.072.

[35] L. Öhrström, I. Michaud-Soret, Fe−Catecholate and Fe−Oxalate Vibrations and Isotopic Substitution Shifts from DFT Quantum Chemistry, J Phys Chem A. 103 (1999) 256–264. https://doi.org/10.1021/jp981508f.

[36] J. Makuraza, Vibrational and Electronic Spectra of Natural Dyes Constituents for Solar Cell Application: DFT and TDDFT Study, International Journal of Materials Science and Applications. 4 (2015) 314. https://doi.org/10.11648/j.ijmsa.20150405.16.

[37] T.L. Valerio, G.A.R. Maia, L.F. Gonçalves, A. Viomar, E. do Prado Banczek, P.R.P. Rodrigues, Study of the Nb2O5 Insertion in ZnO to Dye-sensitized Solar Cells, Materials Research. 22 (2019). https://doi.org/10.1590/1980-5373-MR-2018-0864.

[38] Z. Talebpour, H.R. Bijanzadeh, S. Haghgoo, M. Shamsipur, 1H NMR method for simultaneous identification and determination of caffeine and theophylline in human serum and pharmaceutical preparations, Chem Analityczna. 49 (2004).

[39] Z. Talebpour, S. Haghgoo, M. Shamsipur, 1H nuclear magnetic resonance spectroscopy analysis for simultaneous determination of levodopa, carbidopa and methyldopa in human serum and pharmaceutical formulations, Anal Chim Acta. 506 (2004) 97–104. https://doi.org/10.1016/j.aca.2003.10.081.

[40] A.-V. Lupaescu, C.S. Mocanu, G. Drochioiu, C.-I. Ciobanu, Zinc Binding to NAP-Type Neuroprotective Peptides: Nuclear Magnetic Resonance Studies and Molecular Modeling, Pharmaceuticals. 14 (2021) 1011. https://doi.org/10.3390/ph14101011.

[41] F. Kratz, B. Elsadek, Clinical impact of serum proteins on drug delivery, Journal of Controlled Release. 161 (2012). https://doi.org/10.1016/j.jconrel.2011.11.028.

[42] É.A. Enyedy, L. Horváth, A. Hetényi, T. Tuccinardi, C.G. Hartinger, B.K. Keppler, T. Kiss, Interactions of the carrier ligands of antidiabetic metal complexes with human serum albumin: A combined spectroscopic and separation approach with molecular modeling studies, Bioorg Med Chem. 19 (2011). https://doi.org/10.1016/j.bmc.2011.05.063.

[43] W. Bal, M. Sokołowska, E. Kurowska, P. Faller, Binding of transition metal ions to albumin: Sites, affinities and rates, Biochim Biophys Acta Gen Subj. 1830 (2013). https://doi.org/10.1016/j.bbagen.2013.06.018.

[44] V.R. Martínez, E.G. Ferrer, P.A. Williams, Candesartan, losartan and valsartan Zn(II) complexes interactions with bovine serum albumin, Future Med Chem. 14 (2022) 9–16. https://doi.org/10.4155/fmc-2021-0216.

[45] V.R. Martínez, M. V. Aguirre, J.S. Todaro, E.G. Ferrer, P.A.M. Williams, Improvement of the Anticancer Activities of Telmisartan by Zn(II) Complexation and Mechanisms of Action, Biol Trace Elem Res. 197 (2020) 454–463. https://doi.org/10.1007/s12011-019-02013-w.

[46] Joseph R. Lakowicz, Principles of Fluorescence Spectroscopy, 2013.

[47] M.J. Sever, J.J. Wilker, Visible absorption spectra of metal–catecholate and metal–tironate complexes, Dalton Trans. 4 (2004) 1061–1072. https://doi.org/10.1039/B315811J.

[48] P.D. Ross, S. Subramanian, Thermodynamics of protein association reactions: forces contributing to stability, Biochemistry. 20 (1981) 3096–3102. https://doi.org/10.1021/bi00514a017.

[49] G. Dragusha, B. Zahiti, D. Gorani, F. Gashi, Echocardiografic and biochemic parameter's changes in hypertensive patients treated with methyldopa and lysinopril, HealthMED. 4 (2010).

[50] F.M. Fouad, Y. Nakashima, R.C. Tarazi, E.E. Salcedo, Reversal of left ventricular hypertrophy in hypertensive patients treated with methyldopa, Am J Cardiol. 49 (1982) 795–801. https://doi.org/10.1016/0002-9149(82)91961-0.

[51] R.J. Tomanek, Selective effects of alpha-methyldopa on myocardial cell components independent of cell size in normotensive and genetically hypertensive rats., Hypertension. 4 (1982) 499–506. https://doi.org/10.1161/01.HYP.4.4.499.

[52] E. Dubois-Deruy, V. Peugnet, A. Turkieh, F. Pinet, Oxidative Stress in Cardiovascular Diseases, Antioxidants. 9 (2020) 864. https://doi.org/10.3390/antiox9090864.

[53] M. Toljic, A. Egic, J. Munjas, N. Karadzov Orlic, Z. Milovanovic, A. Radenkovic, J. Vuceljic, I. Joksic, Increased oxidative stress and cytokinesis-block micronucleus cytome assay parameters in pregnant women with gestational diabetes mellitus and gestational arterial hypertension, Reproductive Toxicology. 71 (2017) 55–62. https://doi.org/10.1016/j.reprotox.2017.04.002.

[54] G. Chen, R. Wilson, G. Cumming, W.E. Smith, W.D. Fraser, J.J. Walker, J.H. Mckillop, Effects of Atenolol, Labetalol and Methyldopa on Endogenous Antioxidants In-vitro, Journal of Pharmacy and Pharmacology. 47 (2011) 42–45. https://doi.org/10.1111/j.2042-7158.1995.tb05731.x.

[55] A. Ahmad, S. Dempsey, Z. Daneva, M. Azam, N. Li, P.-L. Li, J. Ritter, Role of Nitric Oxide in the Cardiovascular and Renal Systems, Int J Mol Sci. 19 (2018) 2605. https://doi.org/10.3390/ijms19092605.

[56] S. Umar, A. van der Laarse, Nitric oxide and nitric oxide synthase isoforms in the normal, hypertrophic, and failing heart, Mol Cell Biochem. 333 (2010) 191–201. https://doi.org/10.1007/s11010-009-0219-x.

[57] E. Schulz, T. Gori, T. Münzel, Oxidative stress and endothelial dysfunction in hypertension, Hypertension Research. 34 (2011) 665–673. https://doi.org/10.1038/hr.2011.39.

[58] J.A. Giovannitti, S.M. Thoms, J.J. Crawford, Alpha-2 Adrenergic Receptor Agonists: A Review of Current Clinical Applications, Anesth Prog. 62 (2015) 31–38. https://doi.org/10.2344/0003-3006-62.1.31.

[59] A. Lymperopoulos, G. Rengo, W.J. Koch, Adrenergic Nervous System in Heart Failure, Circ Res. 113 (2013) 739–753. https://doi.org/10.1161/CIRCRESAHA.113.300308.

[60] S. Cotecchia, C.D. del Vescovo, M. Colella, S. Caso, D. Diviani, The alpha1-adrenergic receptors in cardiac hypertrophy: Signaling mechanisms and functional implications, Cell Signal. 27 (2015) 1984–1993. https://doi.org/10.1016/j.cellsig.2015.06.009.

[61] X. Weng, H. Liu, X. Zhang, Q. Sun, C. Li, M. Gu, Y. Xu, S. Li, W. Li, J. Du, An α_2-adrenoceptor agonist: Dexmedetomidine induces protective cardiomyocyte hypertrophy through mitochondrial-AMPK pathway, Int J Med Sci. 17 (2020) 2454–2467. https://doi.org/10.7150/ijms.47598.

[62] R. Gilsbach, J. Schneider, A. Lother, S. Schickinger, J. Leemhuis, L. Hein, Sympathetic 2-adrenoceptors prevent cardiac hypertrophy and fibrosis in mice at baseline but not after chronic pressure overload, Cardiovasc Res. 86 (2010) 432–442. https://doi.org/10.1093/cvr/cvq014.

[63] J. Motiejunaite, L. Amar, E. Vidal-Petiot, Adrenergic receptors and cardiovascular effects of catecholamines, Ann Endocrinol (Paris). 82 (2021) 193–197. https://doi.org/10.1016/j.ando.2020.03.012.

[64] K. Tang, B. Zhong, Q. Luo, Q. Liu, X. Chen, D. Cao, X. Li, S. Yang, Phillyrin attenuates norepinephrine-induced cardiac hypertrophy and inflammatory response by suppressing p38/ERK1/2 MAPK and AKT/NF-kappaB pathways, Eur J Pharmacol. 927 (2022) 175022. https://doi.org/10.1016/j.ejphar.2022.175022.

[65] T.A. Marino, M. Cassidy, D.R. Marino, N.L. Carson, S. Houser, Norepinephrine-induced cardiac hypertrophy of the cat heart, Anat Rec. 229 (1991) 505–510. https://doi.org/10.1002/ar.1092290411.

[66] I. Gavras, Role of α2-adrenergic receptors in hypertension, Am J Hypertens. 14 (2001) S171–S177. https://doi.org/10.1016/S0895-7061(01)02085-4.

[67] Y. Wu, L. Zeng, S. Zhao, Ligands of Adrenergic Receptors: A Structural Point of View, Biomolecules. 11 (2021) 936. https://doi.org/10.3390/biom11070936.

[68] J. Ciolek, A. Maïga, E. Marcon, D. Servent, N. Gilles, Pharmacological characterization of zinc and copper interaction with the human alpha1A-adrenoceptor, Eur J Pharmacol. 655 (2011) 1–8. https://doi.org/10.1016/j.ejphar.2010.12.042.

[69] X. Chen, Y. Xu, L. Qu, L. Wu, G.W. Han, Y. Guo, Y. Wu, Q. Zhou, Q. Sun, C. Chu, J. Yang, L. Yang, Q. Wang, S. Yuan, L. Wang, T. Hu, H. Tao, Y. Sun, Y. Song, L. Hu, Z.-J. Liu, R.C. Stevens, S. Zhao, D. Wu, G. Zhong, Molecular Mechanism for Ligand Recognition and Subtype Selectivity of α2C Adrenergic Receptor, Cell Rep. 29 (2019) 2936-2943.e4. https://doi.org/10.1016/j.celrep.2019.10.112.

[70] M. Neri, D. Cerretani, A.I. Fiaschi, P.F. Laghi, P.E. Lazzerini, A.B. Maffione, L. Micheli, G. Bruni, C. Nencini, G. Giorgi, S. D'Errico, C. Fiore, C. Pomara, I. Riezzo, E. Turillazzi, V. Fineschi, Correlation between cardiac oxidative stress and myocardial pathology due to acute and chronic norepinephrine administration in rats, J Cell Mol Med. 11 (2007) 156–170. https://doi.org/10.1111/j.1582-4934.2007.00009.x.

[71] S.J. Thandapilly, X.L. Louis, T. Yang, D.M. Stringer, L. Yu, S. Zhang, J. Wigle, E. Kardami, P. Zahradka, C. Taylor, H.D. Anderson, T. Netticadan, Resveratrol prevents norepinephrine induced hypertrophy in adult rat cardiomyocytes, by activating NO-AMPK pathway, Eur J Pharmacol. 668 (2011) 217–224. https://doi.org/10.1016/j.ejphar.2011.06.042.

[72] H. Yanagisawa, T. Miyazaki, M. Nodera, Y. Miyajima, T. Suzuki, T. Kido, M. Suka, Zinc-excess intake causes the deterioration of renal function accompanied by an elevation in systemic blood pressure primarily through superoxide radical-induced oxidative stress, Int J Toxicol. 33 (2014). https://doi.org/10.1177/1091581814532958.

[73] H.C. Shih, T.H. Lee, S.C. Chen, C.Y. Li, T. Shibuya, Anti-hypertension effects of traditional Chinese medicine Ju-Ling-Tang on renal hypertensive rats, American Journal of Chinese Medicine. 33 (2005). https://doi.org/10.1142/S0192415X05003545.

[74] M. Szulc, R. Kujawski, P. Mikołajczak, A. Bogacz, M. Wolek, A. Górska, K. Czora-Poczwardowska, M. Ożarowski, A. Gryszczyńska, J. Baraniak, M. Kania-Dobrowolska, A. Adamczak, E. Iwańczyk-Skalska, P.P. Jagodziński, B. Czerny, A. Kamiński, I. Uzar, A. Seremak-Mrozikiewicz, Combined Effects of Methyldopa and Baicalein or Scutellaria baicalensis Roots Extract on Blood Pressure, Heart Rate, and Expression of Inflammatory and Vascular Disease-Related Factors in Spontaneously Hypertensive Pregnant Rats, Pharmaceuticals. 15 (2022). https://doi.org/10.3390/ph15111342.

[75] R.D. Sanders, M. Maze, Alpha2-agonists and other sedatives and amnestics, in: Anesthetic Pharmacology, 2011. https://doi.org/10.1017/cbo9780511781933.031.

Author Statement Agustin Actis Dato: conceptualization, methodology, software, data curation. Valeria R. Martinez: methodology, data curation, writing-original draft review and editing. Jorge O. Velez Rueda: methodology and data curation. Enrique L. Portiansky: conceptualization, methodology, writing-review and editing. Verónica De Giusti; methodology writing-review and editing. Evelina G. Ferrer: conceptualization, methodology, writing-review and editing. Patricia A.M Williams: conceptualization, methodology, writing original draft-review and editing, supervision.

Declaration of interests

☒ The authors declare that they have no known competing financial interests or personal relationships that could have appeared to influence the work reported in this paper.

☐The authors declare the following financial interests/personal relationships which may be considered as potential competing interests:

Highlights

- The Zn-α-methyldopa complex (ZnMD) has been synthesized and characterized.

  Compared to MD:

- It showed similar moderate spontaneous interaction with BSA
- It improved the antihypertensive action.
- It is significantly more effective in the prevention of cardiac hypertrophy and fibrosis.
- It negatively regulates ROS production more effectively than MD alone.